Supporting Information

A Combined Operando Synchrotron X-ray Absorption Spectroscopy and First-Principles Density Functional Theory Study to Unravel the Vanadium Redox Paradox in the $Na_3V_2(PO_4)_2F_3$–$Na_3V_2(PO_4)_2FO_2$ Compositions

Long H. B. Nguyen,[†,‡,§] *Antonella Iadecola,*[§] *Stéphanie Belin,*[⁂] *Jacob Olchowka,*[†,§,ǁ] *Christian Masquelier,*[‡,§,ǁ] *Dany Carlier,*[†,§,ǁ] and *Laurence Croguennec**[,†,§,ǁ]

[†] CNRS, Univ. Bordeaux, Bordeaux INP, ICMCB, UMR CNRS 5026, F-33600, Pessac, France.

[‡] Laboratoire de Réactivité et Chimie des Solides, UMR CNRS 7314, Université de Picardie Jules Verne, F-80039 Amiens Cedex 1, France.

[⁂] SOLEIL Synchrotron, F-91192 Gif-sur-Yvette, France.

[§] RS2E, Réseau Français sur le Stockage Electrochimique de l'Energie, FR CNRS 3459, F-80039 Amiens Cedex 1, France.

[ǁ] ALISTORE-ERI European Research Institute, FR CNRS 3104, Amiens, F-80039 Cedex 1, France.

* Corresponding Author: L. Croguennec (Laurence.Croguennec@icmcb.cnrs.fr)

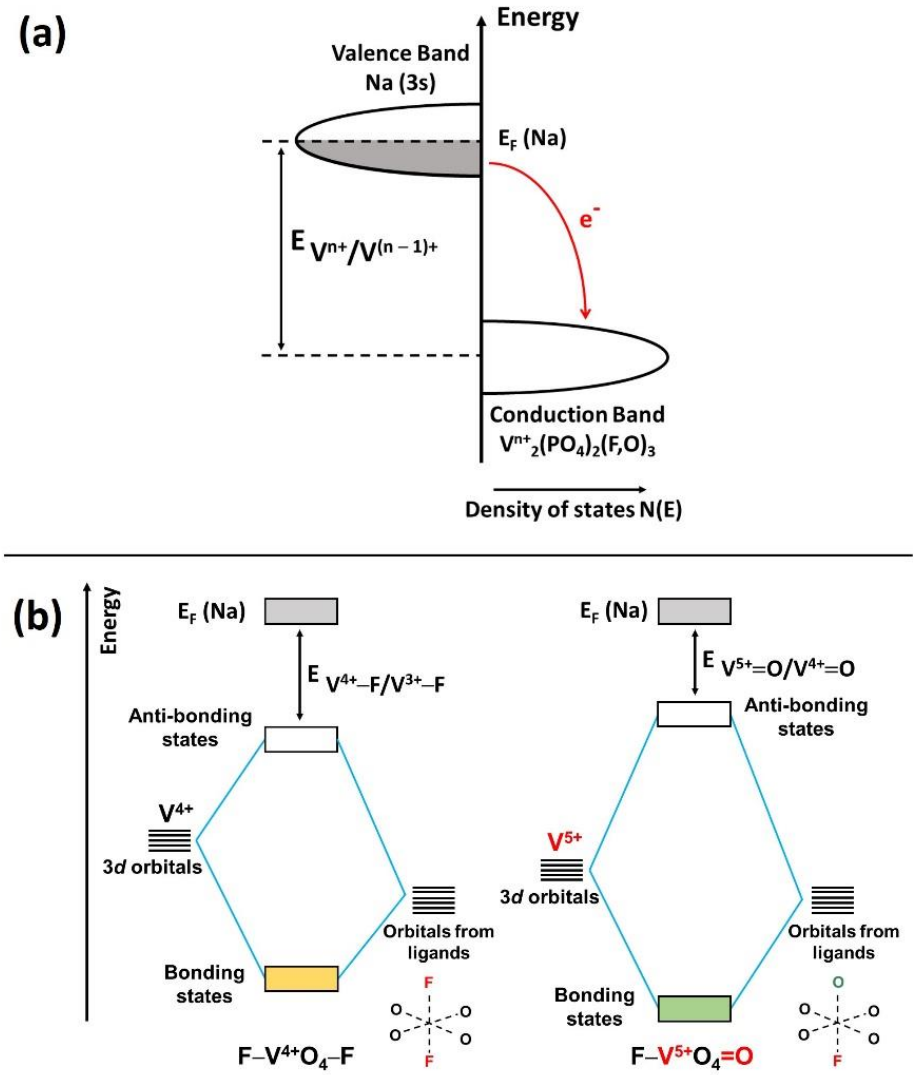

Figure S1: (a) Schematic view showing the position of the $V^{n+}/V^{(n-1)+}$ redox couple in $V^{n+}{}_2(PO_4)_2(F,O)_3$ composition versus Na^+/Na. (b) Molecular diagrams comparing the orbital interactions in F─$V^{4+}O_4$─F and F─$V^{5+}O_4$=O units. The anti-bonding states in F─$V^{5+}O_4$=O are greatly increased due to the presence of the highly covalent vanadyl bond.

In solid-state electrochemistry, the relative position of a redox couple, e.g. F─$V^{4+}O_4$─F/F─$V^{3+}O_4$─F, versus Na^+/Na is defined as the difference between the Fermi level (E_F) of Na metal and the Fermi level of the material containing F─$V^{4+}O_4$─F group, e.g. $NaV_2(PO_4)_2F_3$. The E_F value of $NaV_2(PO_4)_2F_3$ in turn depends strongly on the position of the anti-bonding states resulted from the orbital interaction between V^{4+} and its surrounding ligands. Similar deduction can be made when considering the relative position of the F─$V^{5+}O_4$=O/F─$V^{4+}O_4$=O redox couple versus Na^+/Na. The energy of 3*d* orbitals in an

isolated V^{5+} ion is below the energy of 3*d* orbitals in an isolated V^{4+} ion, and thus anti-bonding states resulted from the V^{5+}─F/O interaction are expected to be localized below the anti-bonding states of the V^{4+}─F/O interaction. Nonetheless, when the V^{5+} ion is involved in a highly covalent vanadyl bond, this strong covalent interaction stabilizes significantly the bonding states, which are occupied by the ligands' electrons, and de-stabilizes greatly the anti-bonding states, which are empty. The energy of the anti-bonding states in $F{-}V^{5+}O_4{=}O$ increases proportionally to the covalency of the vanadyl bond, and lower the gap between these anti-bonding states and the E_F of Na metal.

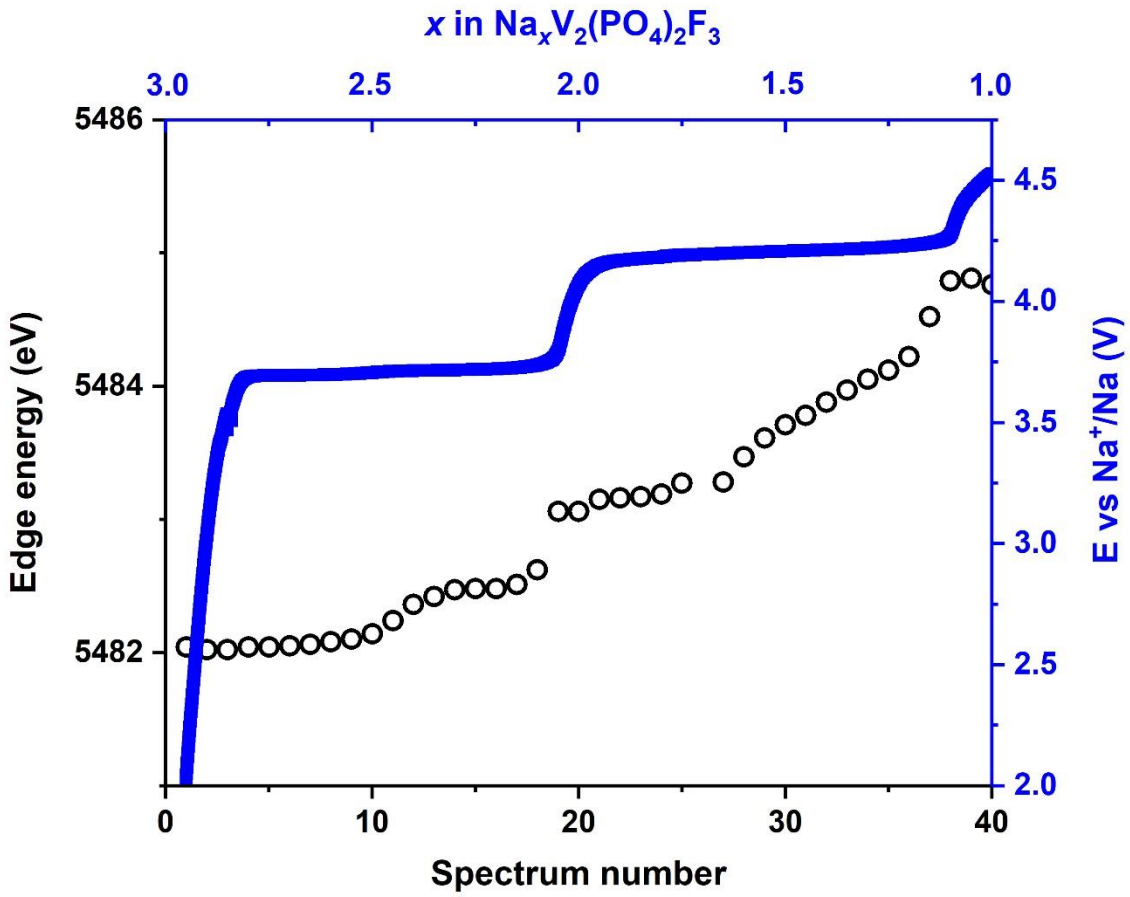

Figure S2: Evolution in the edge energy (taken at normalized absorption equals to 1.0) for the $Na_3V_2(PO_4)_2F_3$─$NaV_2(PO_4)_2F_3$ system. The blue solid line shows the electrochemical profile.

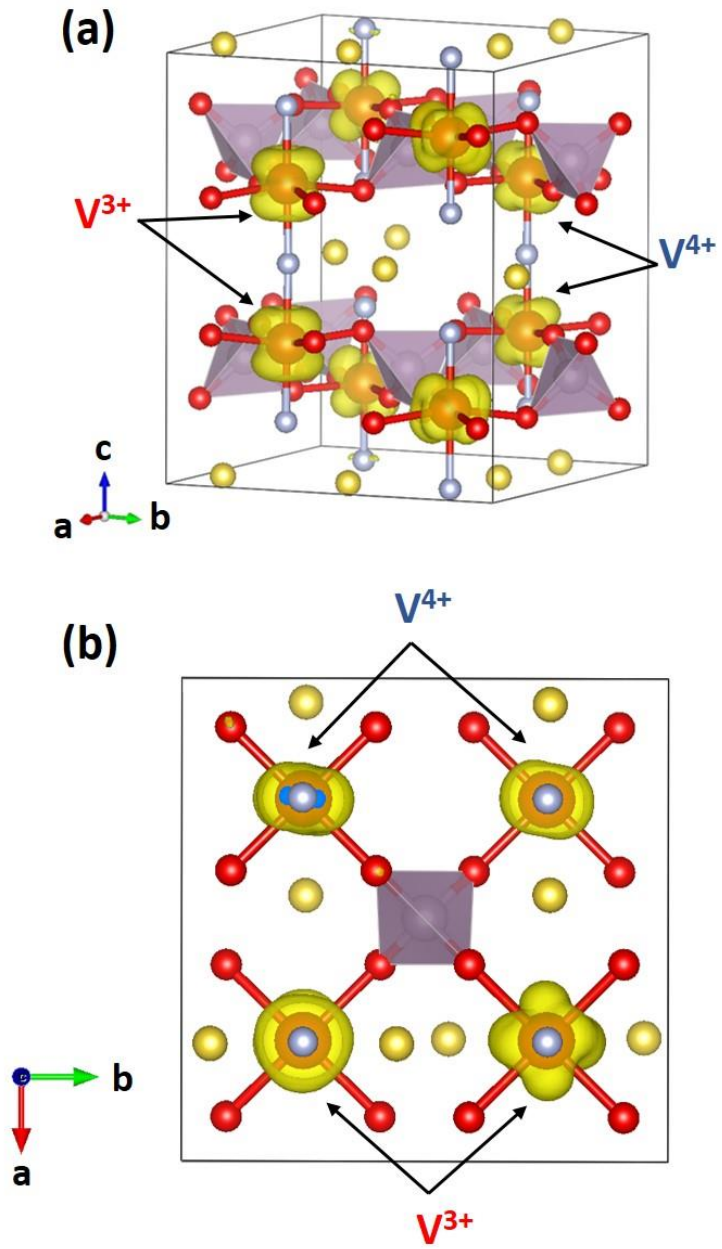

Figure S3: (a) Spin distribution map calculated for $Na_2V_2(PO_4)_2F_3$ using GGA+3.1eV approach with an isosurface value of $1.5 \cdot 10^{-2}$ electron·Å^{-2}.

(b) The projection of the spin distribution map on the (*ab*) plane. The V^{3+} possesses two unpaired electrons, as compared to one unpaired electron of V^{4+}, and thus the orbital lobes of V^{3+} are more extended than those of V^{4+}. The two F─$V^{3+}O_4$─F─$V^{3+}O_4$─F bioctahedra of $Na_2V_2(PO_4)_2F_3$ are not identical due to a slight difference in the Na^+ distribution in their surroundings.

Table S1: V─O/F bond lengths in Vanadium's first coordination sphere obtained from the EXAFS analysis performed on the reconstructed XAS spectra of the three principal components required to describe the *operando* data set recorded on a Na//$Na_3V_2(PO_4)_2F_3$ half-cell upon charging up to 4.5 V vs Na^+/Na.

	Symmetric site	**Distorted site**			
	$d_{V-F/O}$ **(Å)**	d_{V-F} **(Å)**	d_{V-O} **(Å)**	d_{V-F} **(Å)**	**σ (Å²)**
Component 1	2.003(5) × 6				$3.3(5)\cdot10^{-3}$
Component 2	1.967(5) × 6	1.908(5) × 1	1.967(5) × 4	1.746(5) × 1	$6.0(5)\cdot10^{-3}$
Component 3		1.857(5) × 1	1.915(5) × 4	1.726(5) × 1	$6.1(5)\cdot10^{-3}$

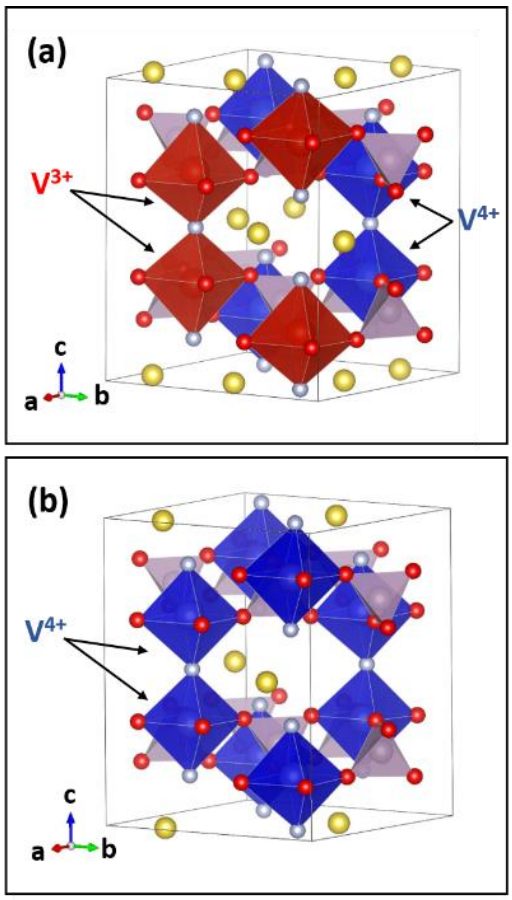

Figure S4: Charge ordering on vanadium sites in (a) $Na_2V_2(PO_4)_2F_3$ and (b) $NaV_2(PO_4)_2F_3$ calculated by first-principles DFT calculations. The $V^{3+}O_4F_2$ and $V^{4+}O_4F_2$ sub-octahedra are represented as red and blue octahedra, respectively. Na^+ ions are represented as yellow spheres.

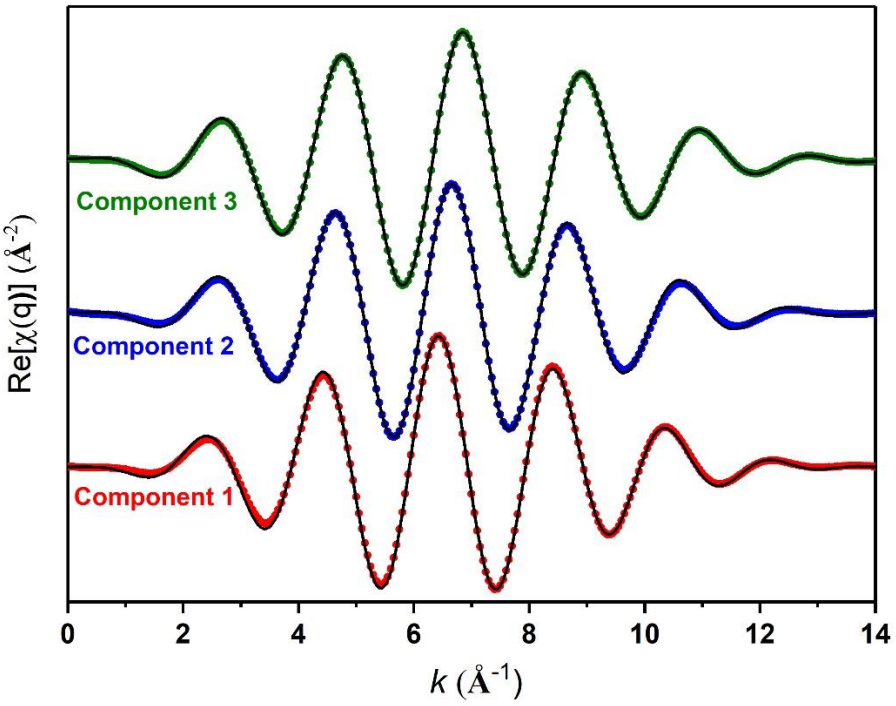

Figure S5: Real part of backward Fourier transform of the EXAFS oscillations $\chi(q)$ of the three principal components of the $Na_3V_2(PO_4)_2F_3$–$NaV_2(PO_4)_2F_3$ system. The backward Fourier transform was considered only in the R-range 1.0 – 2.1 Å with dR = 0 Å (Sine window). The circles represent the experimental data and the solid lines represent the fits.

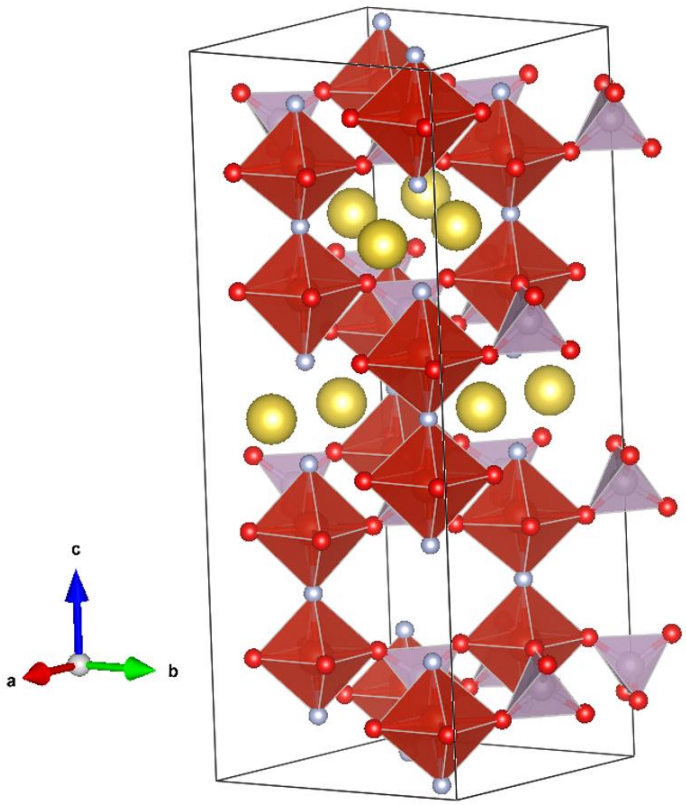

a = 8.95325 Å, b = 8.95382 Å and c = 22.08277 Å

$\alpha = \beta = \gamma = 90^{o}$

Figure S6: Input model for $NaV_2(PO_4)_2F_3$ composition by using a supercell. The supercell was created by doubling the unit cell along the *c* direction and all the Na^+ ions are forced to be distributed in only half of the supercell.

Table S2: V─O/F bond lengths in Vanadium's first coordination sphere obtained from the EXAFS analysis performed on the reconstructed XAS spectra of the three principal components required to describe the *operando* data set recorded on a Na//$Na_3V_2(PO_4)_2F_2O$ half-cell upon charging up to 4.5 V vs Na^+/Na.

	Symmetric site	**Distorted site**			
	$d_{V-F/O}$ **(Å)**	d_{V-F} **(Å)**	d_{V-O} **(Å)**	$d_{V=O}$ **(Å)**	**σ (Å²)**
Component 1	2.033(5) × 6	1.854(5) × 1	1.999(5) × 4	1.629(5) × 1	$3.6(5)\cdot10^{-3}$
Component 2	1.968(5) × 6	1.719(5) × 1	1.974(5) × 4	1.603(5) × 1	$8.0(5)\cdot10^{-3}$
Component 3	1.897(5) × 6	1.731(5) × 1	1.988(5) × 4	1.564(5) × 1	$3.6(5)\cdot10^{-3}$

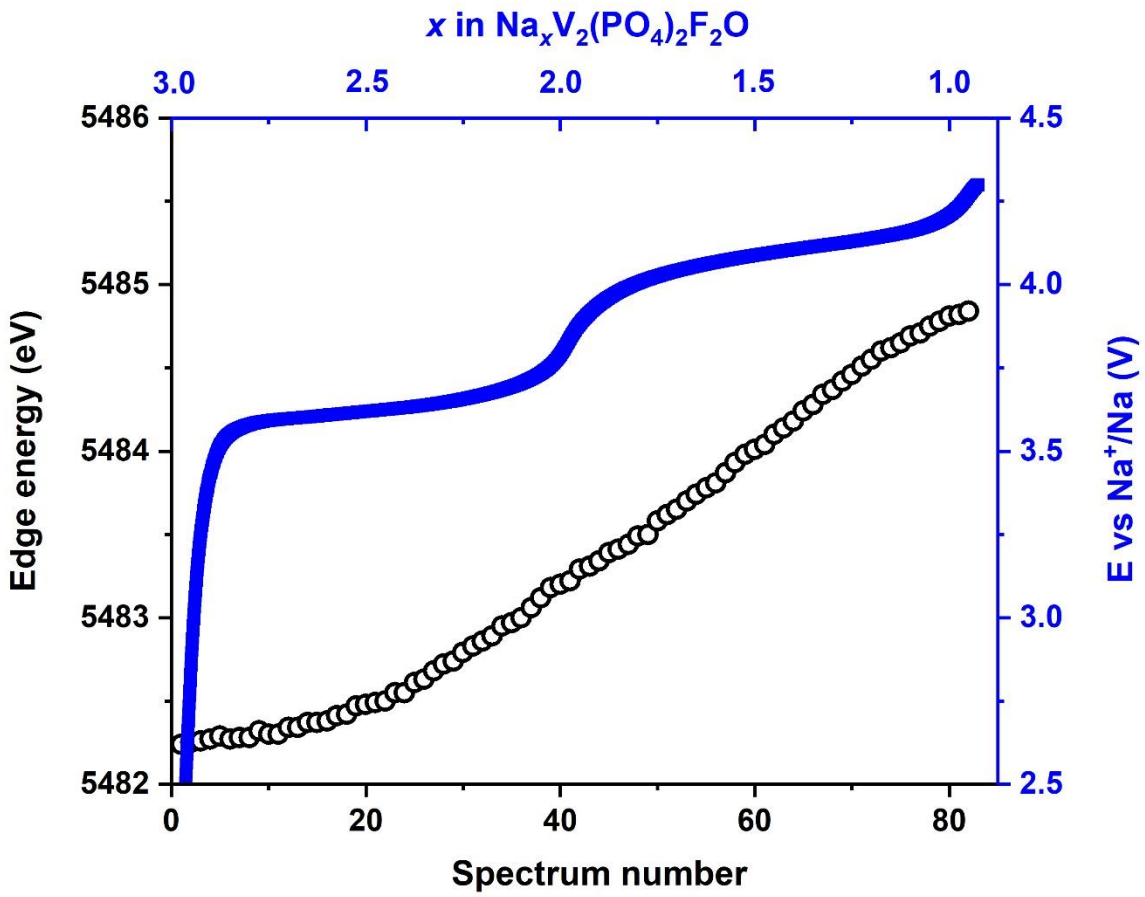

Figure S7: Evolution in the edge energy (taken at normalized absorption equals to 1.0) for the $Na_3V_2(PO_4)_2F_2O$─$NaV_2(PO_4)_2F_2O$ system. The blue solid line shows the electrochemical profile.

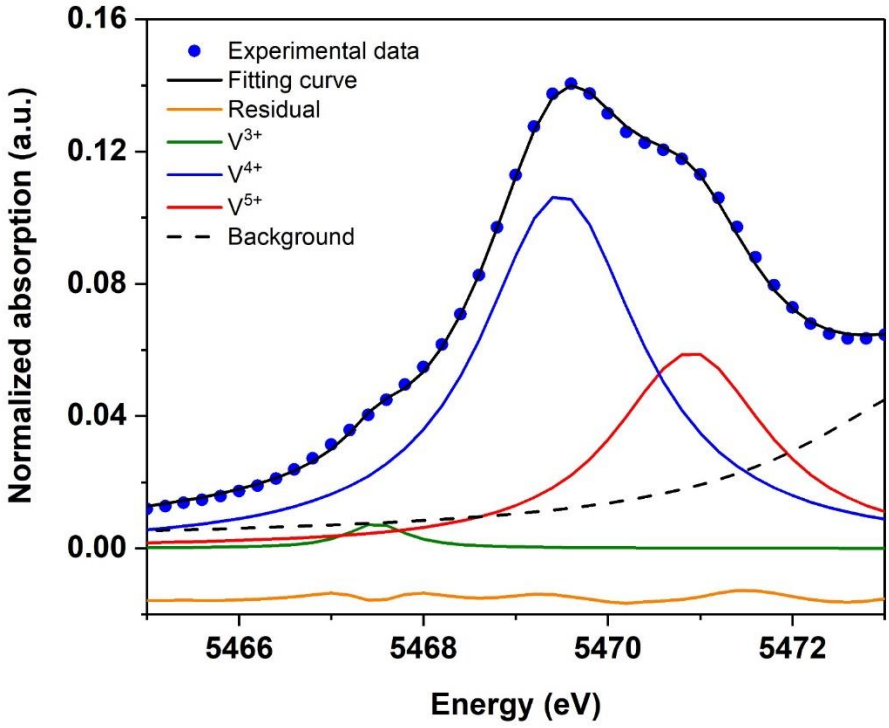

Figure S8: Pre-edge deconvolution on the XANES spectrum #37 recorded *operando* on the $Na_3V_2(PO_4)_2F_2O$─$NaV_2(PO_4)_2F_2O$ system.

The contribution of V^{3+}, V^{4+} and V^{5+} in the pre-edge region are illustrated by green, blue and red curves, respectively.

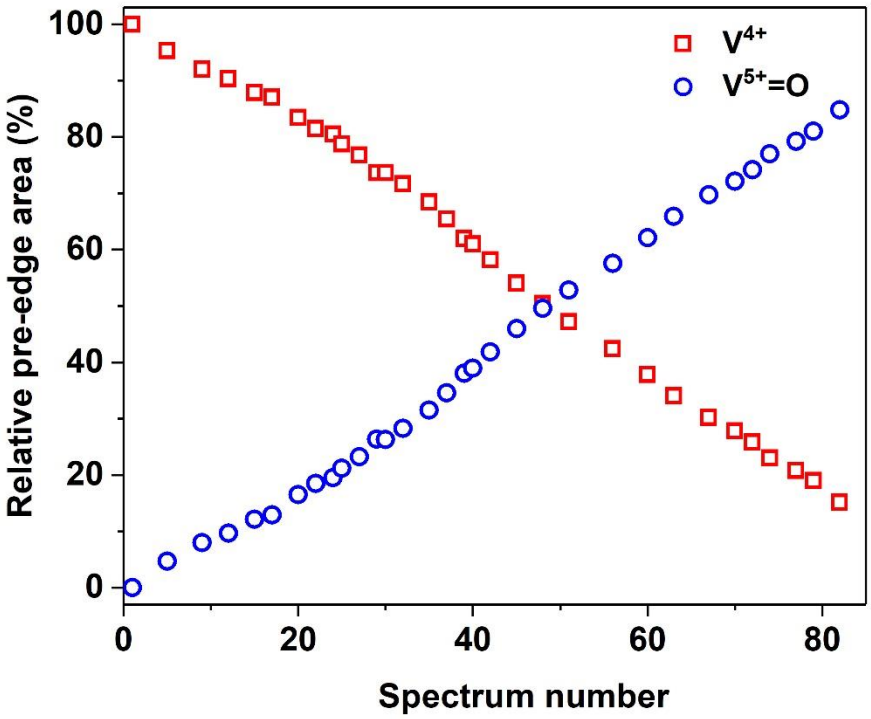

Figure S9: Evolution in the relative area between the two pre-edge signals at 5469.5 eV and 5471.0 eV observed in the $Na_3V_2(PO_4)_2F_2O$—$NaV_2(PO_4)_2F_2O$ system.

The signal at 5469.5 eV corresponds to V^{4+} states (F—$V^{4+}O_4$—F and F—$V^{4+}O_4$=O) while the one at 5471.0 eV corresponds to F—$V^{5+}O_4$=O.

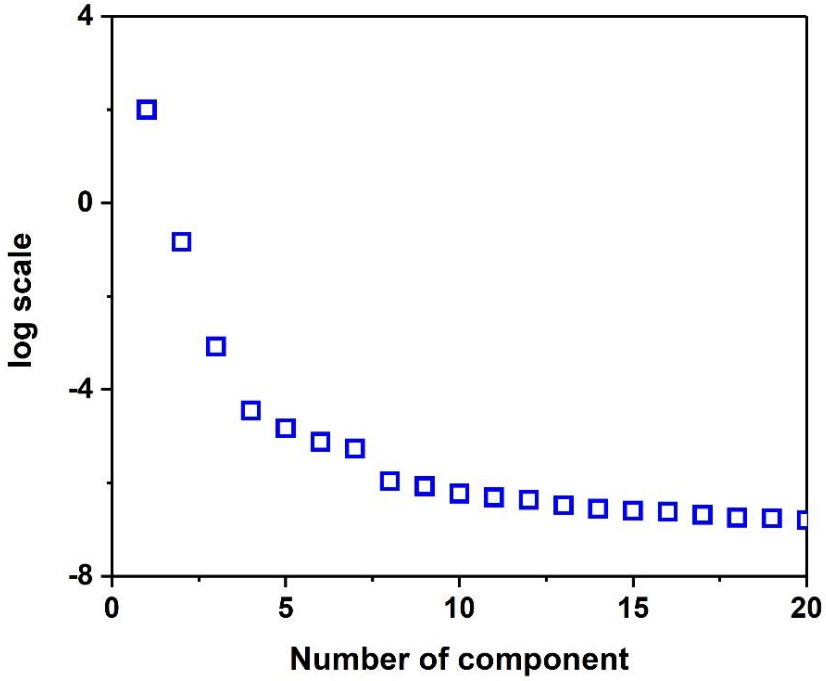

Figure S10: Variance plot of the PCA analysis performed on the *operando* data set recorded on a Na//$Na_3V_2(PO_4)_2F_2O$ half-cell upon charging up to 4.5 V vs Na^+/Na.

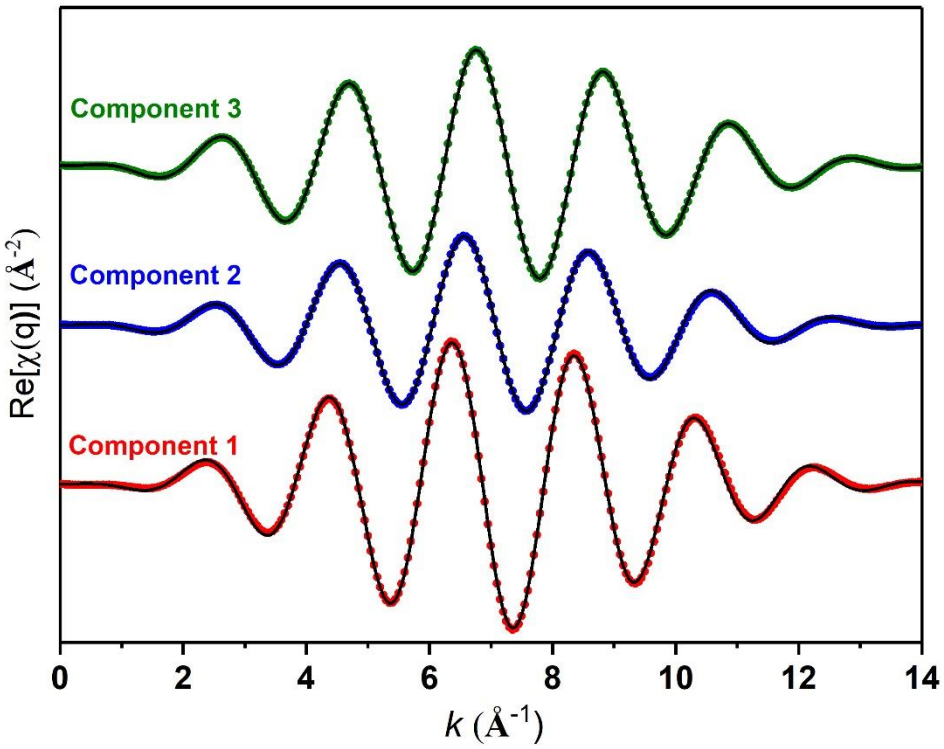

Figure S11: Real part of backward Fourier transform of the EXAFS oscillations $\chi(q)$ of the three principal components of the $Na_3V_2(PO_4)_2F_2O$–$NaV_2(PO_4)_2F_2O$ system. The backward Fourier transform was considered only in the R-range 1.0 – 2.1 Å with dR = 0 Å (Sine window). The circles represent the experimental data and the solid lines represent the fits.

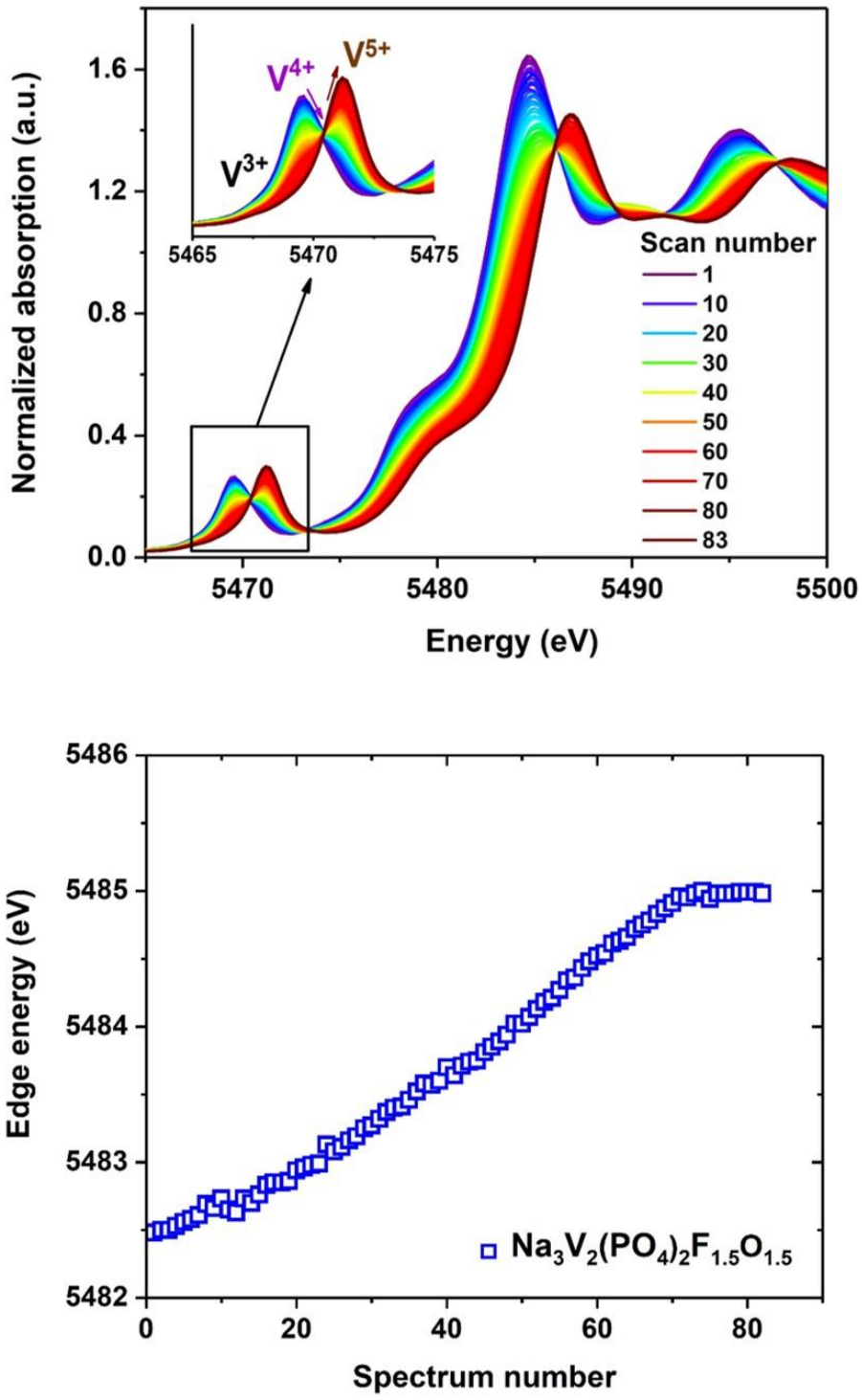

Figure S12: (Top) *Operando* Vanadium K-edge XANES spectra recorded on a $Na//Na_3V_2(PO_4)_2F_{1.5}O_{1.5}$ half-cell from 2.5 to 4.5 V vs Na^+/Na. Inset focuses on the pre-edge. (Bottom) Evolution in the edge energy (taken at normalized absorption equals to 1.0) for the $Na_3V_2(PO_4)_2F_{1.5}O_{1.5}$─$NaV_2(PO_4)_2F_{1.5}O_{1.5}$ system.

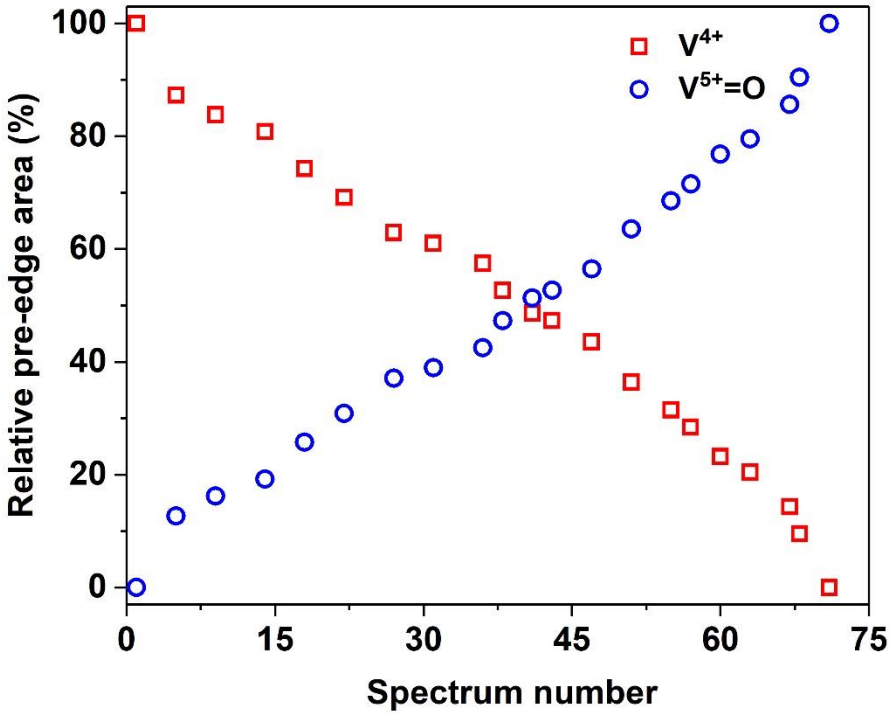

Figure S13: Evolution in the relative area between the two pre-edge signals at 5469.5 eV and 5471.0 eV observed in the $Na_3V_2(PO_4)_2F_{1.5}O_{1.5}$—$NaV_2(PO_4)_2F_{1.5}O_{1.5}$ system. The signal at 5469.5 eV corresponds to V^{4+} states (F—$V^{4+}O_4$—F and F—$V^{4+}O_4$=O) while the one at 5471.0 eV corresponds solely to F—$V^{5+}O_4$=O.

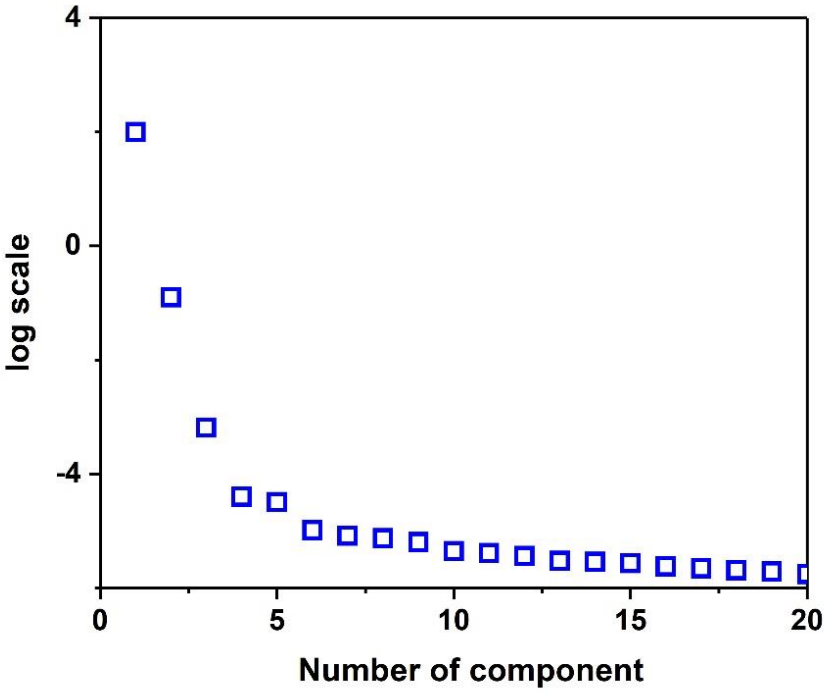

Figure S14: Variance plot of the PCA analysis performed on the *operando* data set recorded on a Na//$Na_3V_2(PO_4)_2F_{1.5}O_{1.5}$ half-cell upon charging up to 4.5 V vs Na^+/Na.

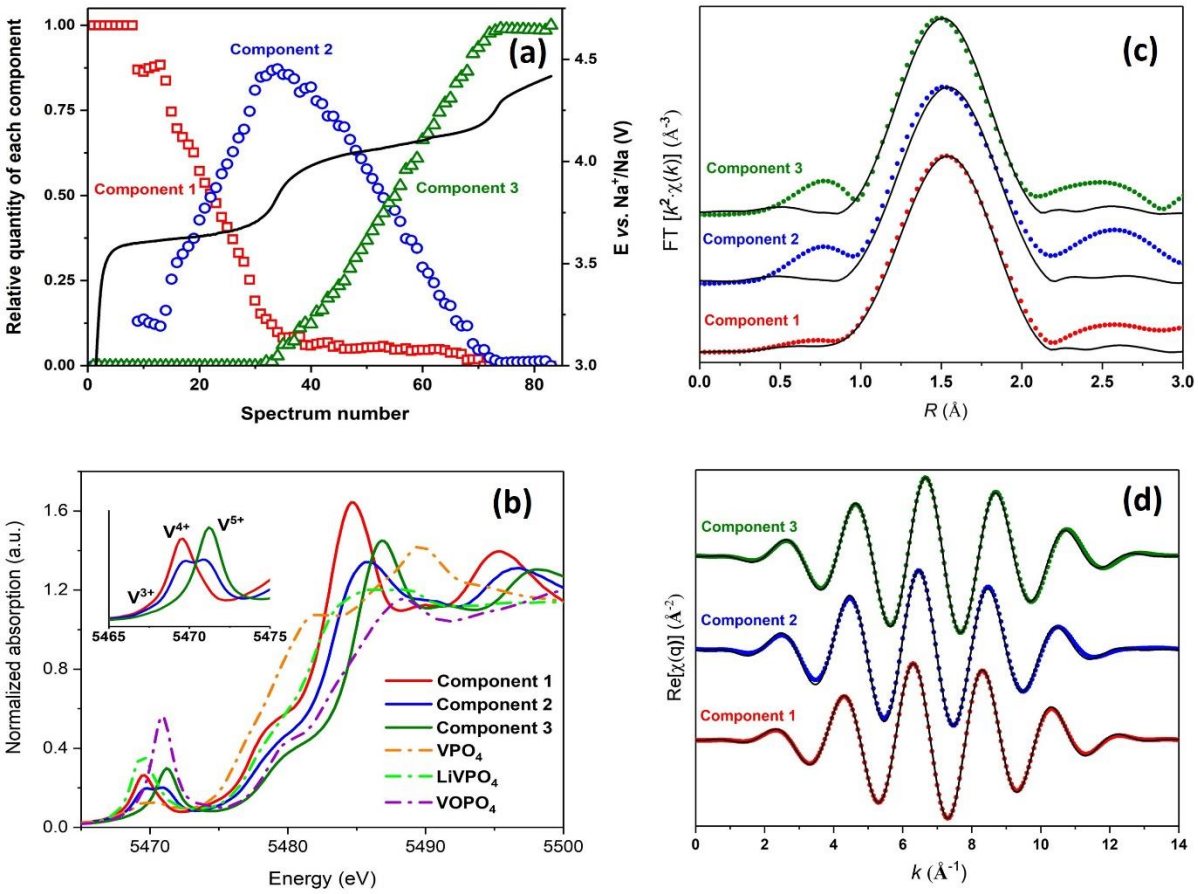

Figure S15: (*a*) Concentration profile of the three principal components required to describe the *operando* XAS spectra recorded on a Na//$Na_3V_2(PO_4)_2F_{1.5}O_{1.5}$ half-cell upon charging from 2.5 to 4.5 V vs Na^+/Na. The corresponding electrochemical profile is shown as black solid curve; (*b*) Reconstructed XANES spectra of the three independent components in the $Na_3V_2(PO_4)_2F_{1.5}O_{1.5}$ – $NaV_2(PO_4)_2F_{1.5}O_{1.5}$ system as compared to the references VPO_4, $LiVOPO_4$ and $VOPO_4$. Inset focuses on the pre-edge area of the reconstructed spectra; (*c*) Fit of the k^2-weighted Vanadium K-edge EXAFS spectrum Fourier transform (*k*-range: 2.7 – 11.6 $Å^{-1}$, sine window) in the *R* space (*R*-range :1.0 – 2.1 Å, d*R* = 0, sine window) for the three components determined for the $Na_3V_2(PO_4)_2F_{1.5}O_{1.5}$ - $NaV_2(PO_4)_2F_{1.5}O_{1.5}$ system; (*d*) Real part of backward Fourier transform of the EXAFS oscillations $\chi(q)$ by considering only the *R*-range 1.0 – 2.1 Å with d*R* = 0 Å (Sine window). The circles represent the experimental data and the solid lines represent the fits.

Table S3: V─O/F bond lengths in Vanadium's first coordination sphere obtained from the EXAFS analysis performed on the reconstructed XAS spectra of the three principal components required to describe the *operando* data set recorded on a Na//$Na_3V_2(PO_4)_2F_{1.5}O_{1.5}$ half-cell upon charging up to 4.5 V vs Na^+/Na.

	Symmetric site†	**Distorted site†**			
	$d_{V-F/O}$ **(Å)**	d_{V-F} **(Å)**	d_{V-O} **(Å)**	$d_{V=O}$ **(Å)**	**σ (Å²)**
Component 1	1.945(5) × 6	1.854(5) × 1	2.062(5) × 4	1.630(5) × 1	$2.0(5)\cdot10^{-3}$
Component 2	1.911(5) × 6	1.758(5) × 1	2.019(5) × 4	1.591(5) × 1	$4.0(5)\cdot10^{-3}$
Component 3	1.856(5) × 6	1.773(5) × 1	1.981(5) × 4	1.578(5) × 1	$1.6(5)\cdot10^{-3}$

† The V─O/F distances represented on **Figure 3** for the mixed valence sites of $Na_3V_2(PO_4)_2F_{1.5}O_{1.5}$ and $NaV_2(PO_4)_2F_{1.5}O_{1.5}$ are average values with the 1/1 contribution of the symmetric and distorted sites

References:

(1) Masquelier, C.; Croguennec, L. Polyanionic (Phosphates, Silicates, Sulfates) Frameworks as Electrode Materials for Rechargeable Li (or Na) Batteries. *Chem. Rev.* **2013**, *113* (8), 6552−6591. https://doi.org/10.1021/cr3001862.

(2) Manthiram, A. A Reflection on Lithium-ion Batteries Cathode Chemistry. *Nat. Commun.* **2020**, *11* (1), 1550. https://doi.org/10.1038/s41467-020-15355-0.